SCIENTIFIC REP☰RTS

OPEN

Norcorrole as a Delocalized, Antiaromatic System

Jeanet Conradie [1,2], Cina Foroutan-Nejad[3] & Abhik Ghosh [1]

Nickel norcorrole provides an unusual example of a molecule that is strongly antiaromatic according to the magnetic criterion, but which exhibits, according to high-quality DFT calculations, a symmetric, delocalized structure with no difference in bond length between adjacent C_{meso}-C_α bonds. A fragment molecular orbital analysis suggests that these discordant observations are a manifestation of the high stability of the dipyrrin fragments, which retain their electronic and structural integrity even as part of the norcorrole ring system.

Over a dozen years ago, one of us conceptualized norcorrole (H_2Nc) as the smallest, realistic, fully conjugated tetrapyrrole ring system as part of a theoretical exercise (Fig. 1)[1]. Among the more notable conclusions of the study, which employed standard density functional theory (DFT) methods, was that nickel norcorrole (NiNc) should exhibit a slightly domed, but otherwise fully symmetric structure. In other words, the calculations did not indicate any difference in bond length between adjacent C_{meso}-C_α bonds, as is typically observed for antiaromatic porphyrinoids[2–4]. Within a few years thereafter, norcorrole was experimentally realized by Bröring and coworkers in the form of an iron(III)-iodido complex[5]. Subsequently, Kobayashi, Shinokubo, and their coworkers reported a gram-scale synthesis of a nickel *meso*-diarylnorcorrole, clearing the path for wide-ranging investigations of the norcorrole derivatives[6]. Interestingly, the X-ray structure reported by these authors (CCDC: YEQKUC) revealed a planar macrocycle geometry with significant bond length alternation[6]. Furthermore, the experimental ^{1}H NMR spectra and nucleus independent chemical shift (NICS) calculations clearly implicated NiNc as an antiaromatic system[6]. Together, these findings pose an interesting conundrum: although NiNc is antiaromatic according to the magnetic criterion, DFT geometry optimizations indicate a symmetric structure with little or no bond length alternation. While chemical theory does not rule out such a system, delocalized, antiaromatic systems are virtually unknown among real molecules. Presented herein is a detailed DFT investigation aimed at establishing the true equilibrium geometry of NiNc.

Results and Discussion

Geometry optimizations with a variety of exchange-correlation functionals reproduced *all* key geometrical features noted in our earlier study[1]. Figure 2 depicts highlights of the B3LYP[7–9] -D3[10]/STO-TZ2P optimized geometries. The energy minima turned out to be a C_i-symmetric wave conformation for H_2Nc[11] and a C_{2v}-symmetric dome conformation for NiNc. The planar D_{2h} form of NiNc, just 0.03 eV (0.7 kcal/mol) higher in energy relative to the C_{2v} minimum, was found to correspond to the transition state for the bowl inversion process. The optimized geometry parameters for NiNc are in excellent agreement with the X-ray structures of several Ni *meso*-diarylnorcorrole derivatives (including CALQIS, CALQOY, CALQUE[12]; YAFSAC, YAFSEF[13]; REMGOI[14]; Table 1). These structures are either planar or slightly domed, consistent with a soft doming potential, and exhibit minimal bond length alternations, in particular minimal differences (<0.02 Å) between adjacent C_{meso}-C_α bonds. The X-ray structures of certain other NiNc derivatives (YEQKUC[6]; CALRAL[12]; MUJTIW, MUJTOC[15], on the other hand, exhibit larger differences (>0.04 Å) between adjacent C_{meso}-C_α bonds. To this list may be added a slightly saddled CuNc (YEHTOX)[11] and a strongly domed PdNc (YEHTEN)[11] structure, which exhibit an intermediate difference (~0.03 Å) between adjacent C_{meso}-C_α bonds. Significant bond localization has been observed for several NiNc derivatives with strongly conjugating β-substituents such as cyano[15], nitro[16] or amino[17]; these systems are not within the purview of the present study. The overall body of results strongly suggests that although NiNc has a symmetric, delocalized global minimum, bond alternation does correspond to a soft distortion and may manifest itself for certain substitution patterns and crystal environments.

[1]Department of Chemistry, UiT – The Arctic University of Norway, 9037, Tromsø, Norway. [2]Department of Chemistry, University of the Free State, 9300, Bloemfontein, Republic of South Africa. [3]CEITEC – Central European Institute of Technology, Masaryk University, Kamenice 5, CZ, 62500, Brno, Czech Republic. Correspondence and requests for materials should be addressed to J.C. (email: conradj@ufs.ac.nz) or C.F.-N. (email: canyslopus@yahoo.co.uk) or A.G. (email: abhik.ghosh@uit.no)
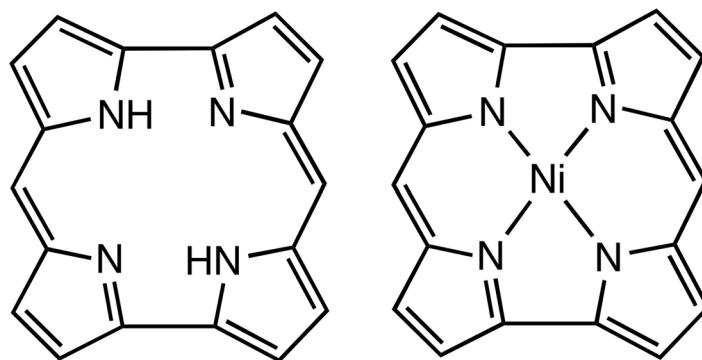
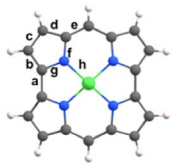**Figure 1.** Free-base (H₂Nc, left) and nickel norcorrole (NiNc, right).
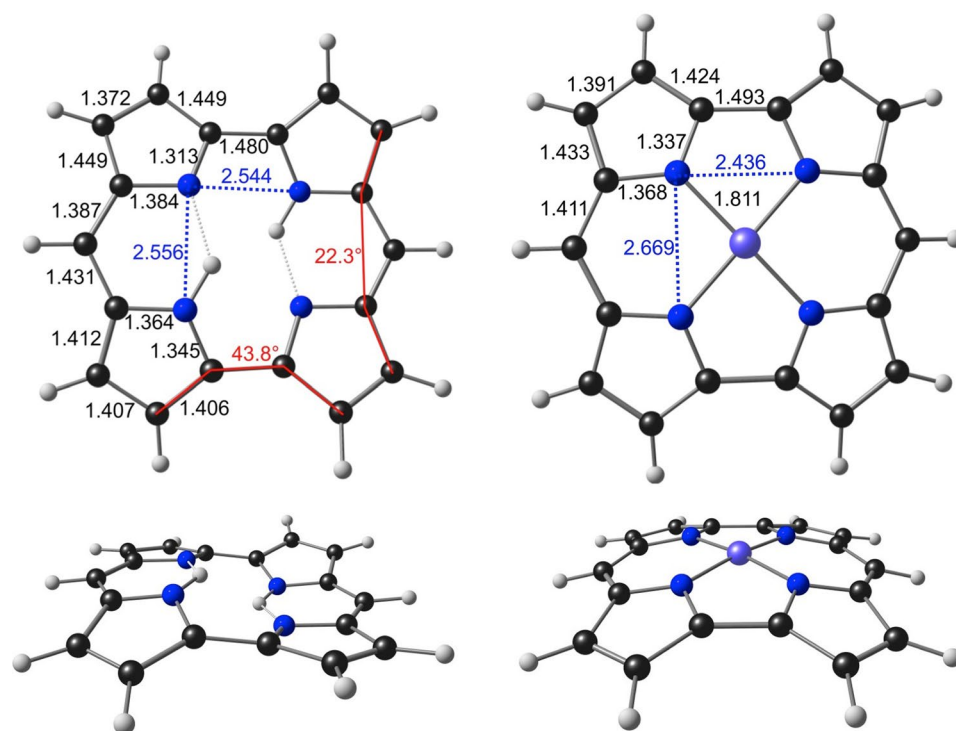
Figure 2. Selected B3LYP-D3/STO-TZ2P geometry parameters (Å, deg) of H₂Nc (left) and NiNc (right).

To investigate the question of magnetic antiaromaticity of NiNc, we visualized the magnetically induced current density profile (as previously done for a variety of porphyrin, hydroporphyrin[18], carbaporphyrin[19], corrole, and isocorrole[20] derivatives) and also calculated the bond magnetizabilities[21,22] at the B3LYP/def2-TZVP[23] level (Fig. 3). Furthermore, we decomposed both the current intensities and the bond magnetizabilities into σ and π components (Table 2). According to the quantum theory of atoms in molecules (QTAIM)[24], the total magnetizability of a closed-shell molecule can be decomposed into atomic and bond magnetizabilities, with the latter providing an indirect measure of the total current density flux through the interatomic surface between two neighboring atoms[25]. Keith and Bader showed that, unlike for aliphatic chains, the atomic and bond magnetizabilities of benzene are significantly anisotropic; the out-of-plane components of the magnetizabilities were found to be about three times larger than the in-plane components[26,27]. In a series of papers, one of us demonstrated that the out-of-plane bond magnetizability provides a safe index for assessing aromaticity even in complicated cases[21,22,28,29], where simple probes such as nucleus independent chemical shift (NICS) and its variants fail[30]. Table 2 shows that the π-framework of NiNc sustains a strong paratropic electronic current (which is associated with positive bond magnetizabilities) that offsets a much smaller diatropic current along the σ–framework. The strong paratropic current is a clear indication of magnetic antiaromaticity of NiNc.

As noted above, nothing in chemical theory actually rules out a delocalized structure for an antiaromatic system. Whether bond localization will occur in a given case depends on the relative importance of π and σ distortivities of the system[31–33]. Typically, for antiaromatic systems, the former wins out[2–4]. The exceptional nature of NiNc in this regard is perhaps best appreciated in terms of the great stability of the two dipyrrin anion (dipy)

| Refcode	Compound	d(M-N)$_{mean}$[a]	d(N-N)$_\parallel$[b]	d(N-N)$_\perp$[c]	D(C$_\alpha$-C$_m$)$_{mean}$[d]	D(C$_\alpha$-N)$_{mean}$[e]	geometry	Metal	Ref
YEHTEN	Palladium *meso,meso*'-dimesitylnorcorrole	1.915	2.533	2.837	0.035	0.011	domed	Pd	[11]
YEHTOX	Copper *meso,meso*'-dimesitylnorcorrole	1.789	2.427	2.628	0.019	0.007	slightly saddled	Cu	[11]
CALQIS	Nickel *meso*-(4-dimethylaminophenyl)-*meso*'-phenylnorcorrole	1.783	2.419	2.618	0.007	0.004	slightly domed	Ni	[12]
CALQOY	Nickel *meso*-(4-dimethylaminophenyl)-*meso*'-phenylnorcorrole	1.782	2.427	2.610	0.003	0.003	planar	Ni	[12]
CALQUE	Nickel *meso*-(4-cyanophenyl)-*meso*'-(4-dimethylaminophenyl)norcorrole	1.771	2.423	2.583	0.000	0.000	planar	Ni	[12]
CALRAL	Nickel *meso*-[3,5-bis(trifluoromethyl)phenyl]-*meso*'-(4-dimethylaminophenyl)norcorrole	1.783	2.422	2.610	0.049	0.018	domed	Ni	[12]
CALRAL	Nickel *meso*-[3,5-bis(trifluoromethyl)phenyl]-*meso*'-(4-dimethylaminophenyl)norcorrole	1.780	2.422	2.611	0.033	0.009	planar	Ni	[12]
CALREP	Nickel *meso*-(4-dimethylaminophenyl)-*meso*'-pentafluorophenylnorcorrole, dichloromethane solvate	1.786	2.425	2.624	0.006	0.021	planar	Ni	[12]
YAFSAC	Nickel *meso,meso*'-diphenylnorcorrole	1.789	2.424	2.614	0.019	0.008	domed	Ni	[13]
YAFSAC	Nickel *meso,meso*'-diphenylnorcorrole	1.779	2.419	2.609	0.019	0.013	slightly waved	Ni	[13]
YEKQUC	Nickel *meso,meso*'-dimesitylnorcorrole	1.779	2.406	2.622	0.044	0.015	planar	Ni	[6]
REMGOI	Nickel 3-(4-dimethylaminophenyl)-5,14-dimesitylnorcorrole), dichloromethane solvate	1.783	2.415	2.621	0.006	0.008	slightly domed	Ni	[14]

Table 1. Selected crystallographic geometry parameters (Å) for relevant norcorrole derivatives. [a]average M-N distance; [b]N…N distances parallel to direct pyrrole-pyrrole bonds; [c]N…N distances perpendicular to direct pyrrole-pyrrole bonds; [d]difference in length between adjacent C$_\alpha$-C$_{meso}$ bonds, averaged over the whole molecule; [e]difference in length between adjacent C$_\alpha$-N bonds, averaged over the whole molecule.

			a	b	c	d	e	f	g	h
	χ_b^{zz}	Total	+23.4	+5.1	+8.6	+5.4	+22.2	+9.3	+15.5	+20.7
		σ	−6.8	−4.8	−3.1	−4.7	−5.7	−3.9	−5.2	−5.7
		π	+30.2	+9.9	+11.7	+10.1	+27.9	+13.2	+20.7	+26.4
	MICI	Total	−61.0	−19.8	−19.5	−19.8	−58.9	−39.1	−41.4	−2.3
		σ	+6.3	+3.6	+11.8	+4.5	−0.4	+2.3	+4.8	+0.3
		π	−67.3	−23.4	−31.3	−24.3	−58.5	−42.4	−46.2	−2.6

Table 2. Out-of-plane bond magnetizabilities (χ_b^{zz}, cgs-ppm) and magnetically induced current intensities (MICI, nA/T) for NiNc. See diagram in the leftmost column for definition of bonds a-h.
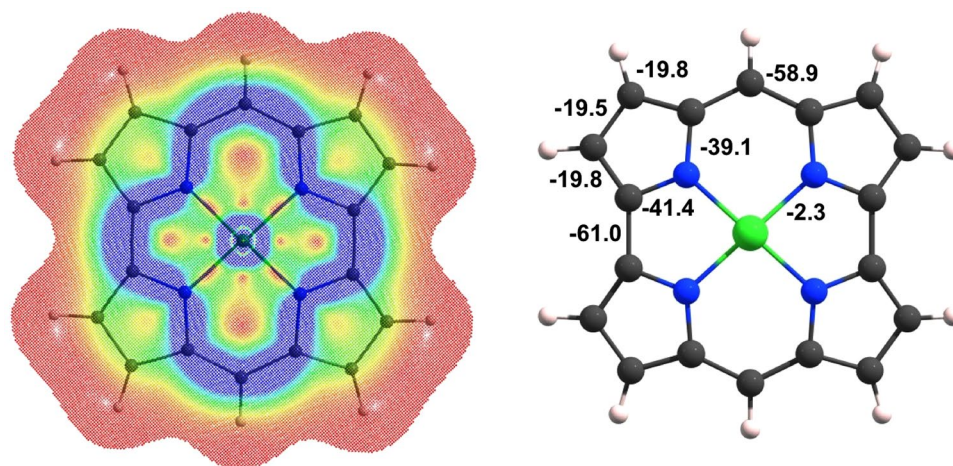
Figure 3. Left: Current density profile of NiNc for a magnetic field applied along the C$_2$ axis of symmetry depicted 1 bohr above the ring plane. Red to blue colors represents weak (0.0 au) to strong (0.001 au) current densities. Right: Integrated current intensities (nA/T).
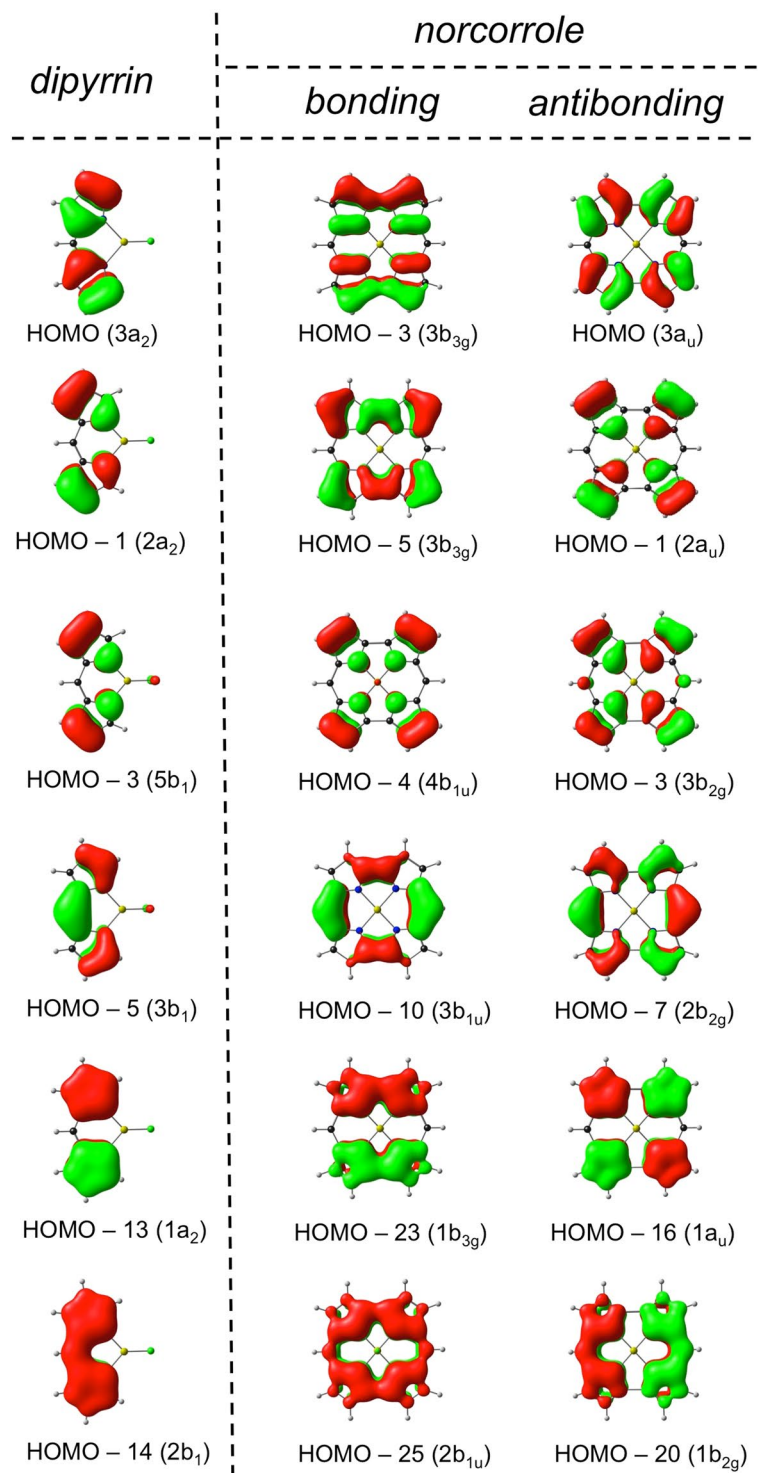
Figure 4. Fragment MO analysis of MgNc in terms of those of Mg(dipy)F.

fragments that make up the molecule. Such an interpretation is fully in line with a fragment molcular orbital (MO) analysis, which we carried out for the planar D_{2h} complex MgNc. As shown in Fig. 4, all 12 occupied π MOs of MgNc may be regarded as bonding and antibonding combinations of the 6 occupied π MOs of the Mg(dipy)F fragments. This statement is actually not a trivial one, the key implication being that none of the occupied π MOs of MgNc owes its origin to any of the *unoccupied* π MOs of the Mg(dipy)F fragments. The two dipyrrin halves thus largely maintain their electronic integrity as part of the norcorrole macrocycle. Notably, such an interpretation is consistent with elementary notions of organic functional groups: as vinylogous amidinates, dipyrrin anions are indeed expected to resist structural distortions such as double bond localization.

Conclusion

Our knowledge of antiaromatic porphyrinoid systems has deepened greatly in recent years. Thus, a variety of spectroscopic features have now been recognized as hallmarks of such systems[34]. As low-bandgap materials, antiaromatic porphyrinoids in general and norcorrole derivatives in particular are potentially of great interest as components of molecular electronic circuits[35]. Against this exciting backdrop, we have confirmed that simple norcorrole derivatives afford unique examples of symmetric, delocalized, antiaromatic systems. Fragment MO analysis suggests that these seemingly contradictory attributes reflect the great stability of the two dipyrrin halves of the molecule. In other words, the energetic imperative of delocalized bonding within the dipyrrin fragments overrules that of antiaromaticity-related bond length alternation.

Methods

Geometry optimization studies and the fragment MO analysis were carried out with the ADF2017[36,37] program system using methods described above. All optimized structures (see Supplementary information for coordinates) were confirmed as local minima via frequency analyses. To obtain current density plots and current intensities, geometry optimizations and GIAO NMR calculations were performed at the B3LYP/def2-TZVP level with Gaussian 09 rev. D1[38]. The NMR computations were further analyzed with the AIMAll (version 16.05.18) suite of programs[39]. Current densities were obtained within the context of quantum theory of atoms in molecules as developed by Keith and Bader[40–44].

References

1. Ghosh, A., Wasbotten, I. H., Davis, W. & Swarts, J. C. Norcorrole and dihydronorcorrole: A predictive quantum chemical study. *Eur. J. Inorg. Chem.* 4479–4485 (2005).
2. Cissell, J. A., Vaid, T. P. & Yap, G. P. The Doubly Oxidized, Antiaromatic Tetraphenylporphyrin Complex [Li(TPP)][BF₄]. *Org. Lett.* **8**, 2401–2404 (2006).
3. Pawlicki, M. & Latos-Grażyński, L. Aromaticity Switching in Porphyrinoids. *Chem. Asian J.* **10**, 1438–1451 (2015).
4. Reddy, B. K., Basavarajappa, A., Ambhore, M. D. & Anand, V. G. Isophlorinoids: The Antiaromatic Congeners of Porphyrinoids. *Chem. Rev.* **117**, 3420–3443 (2017).
5. Bröring, M., Köhler, S. & Kleeberg, C. Norcorrole: Observation of the Smallest Porphyrin Variant with a N₄ Core. *Angew. Chem. Int. Ed.* **47**, 5658–5660 (2008).
6. Ito, T. *et al.* Gram-Scale Synthesis of Nickel(II) Norcorrole: The Smallest Antiaromatic Porphyrinoid. *Angew. Chem. Int. Ed.* **51**, 8542–8545 (2012).
7. Becke, A. D. Density-functional exchange-energy approximation with correct asymptotic behavior. *Phys. Rev. A* **38**, 3098–3100 (1988).
8. Lee, C., Yang, W. & Parr, R. G. Development of the Colle-Salvetti correlation-energy formula into a functional of the electron density. *Phys. Rev. B* **37**, 785–789 (1988).
9. Miehlich, B., Savin, A., Stoll, H. & Preuss, H. Results obtained with the correlation energy density functionals of Becke and Lee, Yang and Parr. *Chem. Phys. Lett.* **157**, 200–206 (1989).
10. Grimme, S., Anthony, J., Ehrlich, S. & Krieg, H. A. A consistent and accurate ab initio parametrization of density functional dispersion correction (DFT-D) for the 94 elements H-Pu. *J. Chem. Phys.* **132**, 154104 (2010).
11. Yonezawa, T., Shafie, S. A., Hiroto, S. & Shinokubo, H. Shaping Antiaromatic π-Systems by Metalation: Synthesis of a Bowl-Shaped Antiaromatic Palladium Norcorrole. *Angew. Chem. Int. Ed.* **56**, 11822–11825 (2017).
12. Yoshida, T., Sakamaki, D., Seki, S. & Shinokubo, H. Enhancing the low-energy absorption band and charge mobility of antiaromatic Niᴵᴵ norcorroles by their substituent effects. *Chem. Commun.* **53**, 1112 (2017).
13. Nozawa, R. *et al.* Stacked antiaromatic porphyrins. *Nat. Comm.* **7**, 13620 (2016).
14. Kawashima, H., Hiroto, S. & Shinokubo, H. Acid-Mediated Migration of Bromide in an Antiaromatic Porphyrinoid: Preparation of Two Regioisomeric Ni(II) Bromonorcorroles. *J. Org. Chem.* **82**, 10425–10432 (2017).
15. Nozawa, R., Yamamoto, K., Shin, J., Hiroto, S. & Shinokubo, H. Regioselective Nucleophilic Functionalization of Antiaromatic Nickel(II) Norcorroles. *Angew. Chem. Int. Ed.* **54**, 8454–8457 (2015).
16. Deng, Z., Li, X., Stępień, M. & Chmielewski, P. J. Nitration of Norcorrolatonickel(II): First Observation of a Diatropic Current in a System Comprising a Norcorrole Ring. *Chem. Eur. J.* **22**, 4231–4246 (2016).
17. Yoshida, T. & Shinokubo, H. Direct amination of the antiaromatic Niᴵᴵ norcorrole. *Mater. Chem. Front.* **1**, 1853–1857 (2017).
18. Fliegl, H. & Sundholm, D. Aromatic Pathways of Porphins, Chlorins, and Bacteriochlorins. *J. Org. Chem.* **77**, 3408–3414 (2012).
19. Ghosh, A., Larsen, S., Conradie, J. & Foroutan-Nejad, C. Local *versus* global aromaticity in azuliporphyrin and benziporphyrin derivatives. *Org. Biomol. Chem.* **16**, 7964–7970 (2018).
20. Foroutan-Nejad, C., Larsen, S., Conradie, J. & Ghosh, A. Isocorroles as Homoaromatic NIR-Absorbing Chromophores: A First Quantum Chemical Study. *Sci. Rep.* **8**, 11952 (2018).
21. Foroutan-Nejad, C. Interatomic Magnetizability: A QTAIM-Based Approach toward Deciphering Magnetic Aromaticity. *J. Phys. Chem. A* **115**, 12555–12560 (2011).
22. Foroutan-Nejad, C. Al₄²⁻: the anion–π interactions and aromaticity in the presence of counter ions. *Phys. Chem. Chem. Phys.* **14**, 9738 (2012).
23. Weigend, F. & Ahlrichs, R. Balanced basis sets of split valence, triple zeta valence and quadruple zeta valence quality for H to Rn: Design and assessment of accuracy. *Phys. Chem. Chem. Phys.* **7**, 3297–3305 (2005).
24. Bader, R. F. W. *Atoms in Molecules: A Quantum Theory*, Clarendon Press, Oxford, New York (1990).
25. Foroutan-Nejad, C., Shahbazian, S. & Marek, R. Toward a Consistent Interpretation of the QTAIM: Tortuous Link between Chemical Bonds, Interactions, and Bond/Line Paths. *Chem. Eur. J.* **20**, 10140–10152 (2014).
26. Bader, R. F. W. & Keith, T. A. Properties of atoms in molecules: Magnetic susceptibilities. *J. Chem. Phys.* **99**, 3683–3693 (1993).
27. Bader, R. F. W. & Keith, T. A. Use of electron charge and current distributions in the determination of atomic contributions to magnetic properties. *Int. J. Quantum Chem.* **60**, 373–379 (1996).
28. Badri, Z. *et al.* All-Metal Aromaticity: Revisiting the Ring Current Model among Transition Metal Clusters. *J. Chem. Theory Comput.* **9**, 4789–4796 (2013).
29. Foroutan-Nejad, C. Is NICS a reliable aromaticity index for transition metal clusters? *Theor. Chem. Acc.* **134**, 8 (2015).
30. Chen, Z., Wannere, C. S., Corminboeuf, C., Puchta, R. & Schleyer, P. V. R. Nucleus-Independent Chemical Shifts (NICS) as an Aromaticity Criterion. *Chem. Rev.* **105**, 3842–3888 (2005).
31. Heilbronner, E. Why do some molecules have symmetry different from that expected? *J. Chem. Educ.* **66**, 471–478 (1989).
32. Shaik, S., Shurki, A., Danovich, D. & Hiberty, P. C. A Different Story of π-Delocalization – The Distortivity of π-Electrons and Its Chemical Manifestations. *Chem. Rev.* **101**, 1501–1539 (2001).

33. Ceulemans, A., Lijnen, E., Fowler, P. W., Mallion, R. B. & Pisanski, T. Graph theory and the Jahn–Teller theorem. *Proc. Roy. Soc. A* 1–19 (2011).
34. Cho, S. *et al.* Defining Spectroscopic Features of Heteroannulenic Antiaromatic Porphyrinoids. *J. Phys. Chem. Lett.* **1**, 895–900 (2010).
35. Fujii, S. *et al.* Highly-conducting molecular circuits based on antiaromaticity. *Nat. Commun.* **8**, 15984 (2017).
36. te Velde, G. *et al.* Chemistry with ADF. *J. Comput. Chem.* **22**, 931–967 (2001).
37. Guerra, C. F., Snijders, J. G., te Velde, G. & Baerends, E. J. Towards an order-N DFT method. *Theor. Chem. Acc.* **99**, 391–403 (1998).
38. Frisch, M. J. *et al. Gaussian 09*, Gaussian, Inc., Wallingford CT (2013).
39. Keith, T. A. *AIMAll*, Gristmill Software: Overland Park KS, USA (2017).
40. Keith, T. A. & Bader, R. F. W. Calculation of magnetic response properties using atoms in molecules. *Chem. Phys. Lett.* **194**, 1–8 (1992).
41. Keith, T. A. & Bader, R. F. W. Calculation of magnetic response properties using a continuous set of gauge transformations. *Chem. Phys. Lett.* **210**, 223–231 (1993).
42. Keith, T. A. & Bader, R. F. W. Topological analysis of magnetically induced molecular current distributions. *J. Chem. Phys.* **99**, 3669–3682 (1993).
43. Keith, T. A. Calculation of magnetizabilities using GIAO current density distributions. *Chem. Phys.* **213**, 123–132 (1996).
44. Keith, T. A. & Bader, R. F. W. Properties of atoms in molecules: nuclear magnetic shielding. *Can. J. Chem.* **74**, 185–200 (1996).

Acknowledgements

Author Contributions

J.C. carried out the MO and TDDFT analyses, C.F.N. performed the current density calculations and A.G. planned and coordinated the project. All authors contributed to the writing of the paper.

Additional Information

Supplementary information accompanies this paper at https://doi.org/10.1038/s41598-019-39972-y.

Competing Interests: The authors declare no competing interests.

Publisher's note: Springer Nature remains neutral with regard to jurisdictional claims in published maps and institutional affiliations.